Available online at www.sciencedirect.com
ScienceDirect
Bioorganic & Medicinal Chemistry Letters 16 (2006) 6226–6230
Bioorganic & Medicinal Chemistry Letters

Xanthine mimetics as potent dipeptidyl peptidase IV inhibitors

Ravi Kurukulasuriya,* Jeffrey J. Rohde, Bruce G. Szczepankiewicz, Fatima Basha, Chunqui Lai, Hwan-Soo Jae, Martin Winn, Kent D. Stewart, Kenton L. Longenecker, Thomas W. Lubben, Stephen J. Ballaron, Hing L. Sham and Thomas W. von Geldern

Metabolic Disease Research, Global Pharmaceutical Research and Development, Abbott Laboratories, 100 Abbott Park Road, Abbott Park, IL 60064-6098, USA

Received 20 July 2006; revised 7 September 2006; accepted 8 September 2006
Available online 28 September 2006

Abstract—A series of xanthine mimetics containing 5,5 and 5,6 heterocycle fused imidazoles were synthesized as dipeptidyl peptidase IV inhibitors. Compound **7** is potent (h-DPPIV K_i = 2 nM) and exhibits excellent selectivity and no species specificity against rat and human enzymes. The X-ray structure confirms that the binding mode of **7** to rat DPPIV is similar to the parent xanthines.

The incretin hormones glucagon like peptide-1 (GLP-1) and glucose dependent insulinotropic polypeptide (GIP) play an important role in glucose homeostasis with effects on the pancreas, gastrointestinal tract, muscle tissue, and brain.[1,2] GLP-1 enhances glucose-stimulated insulin secretion from the β-cells of the pancreas,[3] promotes insulin biosynthesis,[4] and inhibits postprandial glucagon secretion.[5] Administration of GLP-1 reduces the rate of gastric emptying,[6] suppresses appetite and, importantly, promotes β-cell mass.[7] Exenatide, a potent GLP-1 mimetic administered subcutaneously, is currently approved for treatment of type 2 diabetes.[8] Under physiological conditions, the incretin effect is brief because of the short half-life of the incretin hormones due to the action of dipeptidyl peptidase IV (DPPIV) enzyme. DPPIV is a serine protease that cleaves a dipeptide from the N-terminus of the active form of GLP-1, GIP, neuropeptides, and chemokines, and renders them inactive. This discovery has led to the development of DPPIV inhibitors to increase the half-life of circulating incretin hormones and normalize glucose homeostasis.[9] DPPIV has now become a validated target with several small molecule inhibitors in late stage clinical trials for the treatment of type 2 diabetes.[10]

DPPIV inhibitors can be broadly categorized into peptidic and non-peptidic series, with a majority of the inhibitors that have successfully advanced to late stage trials being of peptidyl origin.[10] DPPIV inhibitors related to xanthines include purine, uracil, imidazole, pyrimidine, and pyridine analogs.[11] Each of these subclasses serves as a core to direct key peripheral groups in a direction important to maintain several points of contact needed for potent DPPIV inhibition. Takeda San Diego (formerly Syrrx) recently disclosed SYR-322 which bears a central uracil moiety.[12] SYR-322 was reported to be in phase III clinical trials making it likely that compounds in this class will play an important role in DPPIV inhibition and type 2 diabetes therapy (Fig. 1).

A high throughput screen of the Abbott library of compounds for potential DPPIV inhibitors revealed several xanthine analogs exhibiting low micromolar potency

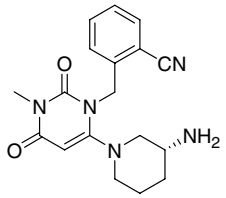

Syr-322

DPPIV IC_{50} = 4 nM

Figure 1. Lead DPPIV inhibitor in late stage clinical trials.

Keywords: Dipeptidyl peptidase IV (DPPIV); Xanthines; SAR; X-ray structure; Type 2 diabetes.
* Corresponding author. Tel.: +1 847 935 5699; e-mail: ravi.kurukulasuriya@abbott.com

0960-894X/$ - see front matter © 2006 Elsevier Ltd. All rights reserved.
doi:10.1016/j.bmcl.2006.09.024

for the enzyme. Preliminary SAR on the xanthine revealed that N-7 alkylation of the xanthine moiety was needed, preferably with a (2-cyano) benzyl group. Substitution at the 8-position was also required with 3-amino piperidine being optimal. N-1 substitution was tolerated but not required. A protein X-ray crystallographic study of the most potent screening lead **6**,[13] bound within the active site of rat DPPIV, was in accordance with these early SAR observations.[14] Groups at the 7- and 8-positions of the xanthine ring system made specific protein contacts. In addition, a hydrogen bond between the 6-carbonyl oxygen and the backbone N–H of Tyr 632 of the protein was observed. Positions 1 and 2 were in close proximity to the protein but had no direct interaction, while N-3 and N-9 appeared to be in a large solvent pocket (Fig. 2).

Based on the X-ray data, we embarked on a synthetic program which targeted xanthine analogs that retain the imidazole and 6-carbonyl moieties but possess alternative **A**-ring heterocycles. We envisioned that such a change would still enable the core to orient the vital N-7 benzylic and the C-8 (3-amino)-piperidine pharmacophores in a similar direction as the xanthine to maintain potent DPPIV inhibition while providing the flexibility to modulate the pharmacokinetic properties of the compounds. To aid the medicinal chemistry strategy, a convergent procedure was developed to obtain 5,5 and 5,6 ring fused xanthine mimetics. A Cu^{I} mediated cyclization utilizing the acyclic guanidine derived from 3-amino piperidine was the key step (Scheme 1).[15] Alkylation at N-7 and deprotection provided DPPIV inhibitor **6**. Related fused imidazole compounds were synthesized by similar procedures.

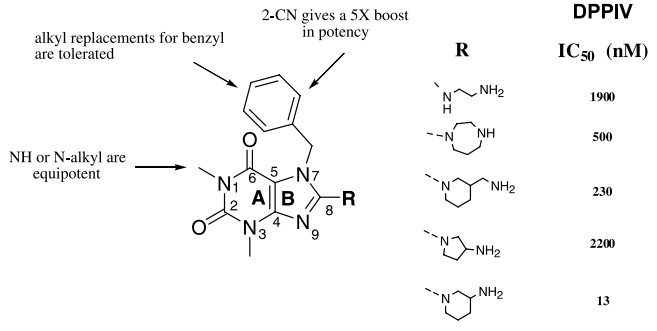

Figure 2. Preliminary SAR on the xanthine hit.

The in vitro activity of the compounds was tested against human and rat DPPIV enzyme. Data for selected compounds are shown in Table 1. Xanthine **6** with an *ortho*-cyano benzyl group off the imidazole (N-7) nitrogen was extremely potent (h-DPPIV $K_i = 2$ nM). The potency is retained when the **A** ring of the xanthine is replaced with a methyl maleimide as in **7** (h-DPPIV $K_i = 2$ nM) or methyl pyridazinone as in **8** (h-DPPIV $K_i = 5$ nM). The *ortho*-cyano group can be substituted with small electron-withdrawing groups such as a chloro as in **9** (h-DPPV $K_i = 9$ nM) or trifluoromethyl as in **10** (h-DPPIV $K_i = 10$ nM) with a 5-fold loss in potency. Larger groups such as a trifluoromethoxy as in **11** (h-DPPIV $K_i = 22$ nM) are less desirable with a 10-fold loss in DPPIV activity compared to **7**. Notably human DPPIV inhibition is dramatically weakened when the *ortho*-cyano group is moved to the *meta*-position as in **12** (h-DPPIV $K_i = 1200$ nM). Modeling of *meta*-substituents indicated that a *meta* acetonitrile as in **13** would allow the cyano group to reorient to be similar to **8**. As modeling predicted, potency was re-established with **13** (h-DPPIV $K_i = 11$ nM). The SAR indicates that both the benzylic moiety and a small electron-withdrawing group (EWG) are important for potent DPPIV inhibition and the optimum orientation for the protein–inhibitor interaction is when the small EWG is at the *ortho*-position of the aryl group. Extended groups at the **A** ring are less desirable. For example, benzyl maleimide as in **14** (h-DPPIV $K_i = 29$ nM) was less potent than methyl maleimide **7**. Similarly naphthoquinone as in **15** (h-DPPIV $K_i = 25$ nM) was less potent than **7**. Not all heterocyclic substitutions at the **A** ring were tolerated. Substitution of the C-6 carbonyl of the uracil moiety of **6** with a fluoro group as in **16** (h-DPPIV $K_i = 57$ nM) diminished potency while a pyridine N-oxide as in **17** (h-DPPIV $K_i = 300$ nM) was weakly active. The location of the C-6 carbonyl group relative to the benzyl moiety off the imidazole is also critical. For example when the *ortho*-cyano benzyl group is attached to the imidazole N-9 nitrogen distal to the carbonyl of the pyridazinone as in **18** (h-DPPIV $K_i = 260$ nM) the potency decreased sharply.

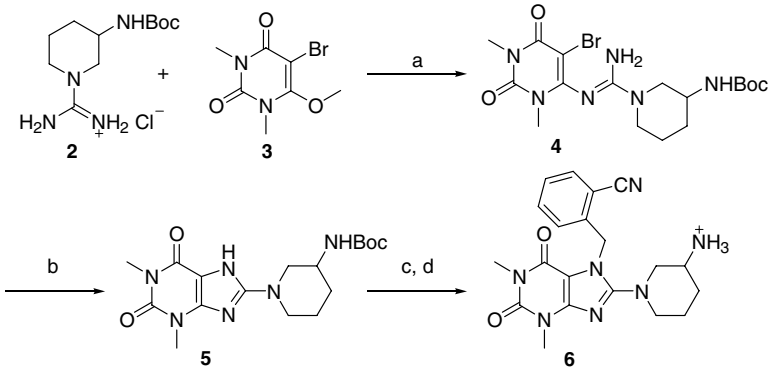

Scheme 1. Reagents and conditions: (a) NaOMe, MeOH, 80 °C, 64%; (b) NaH, CuI, THF, 75 °C, 77%; (c) BnBr, K_2CO_3, DMF, 23 °C, 50%; (d) TFA, CH_2Cl_2, 23 °C, 95%.

Table 1. Human DPPIV binding for selected compounds

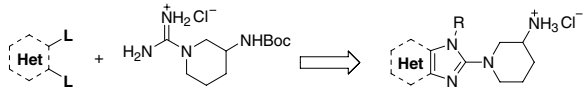

Compound	Het	Product	h-DPPIV K_i (nM)
6	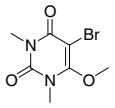	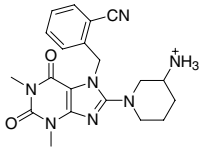	2
7	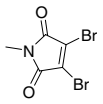	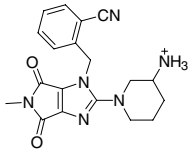	2
8	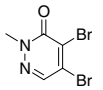	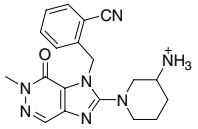	5
9	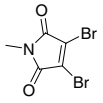	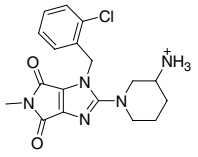	9
10	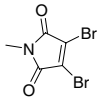	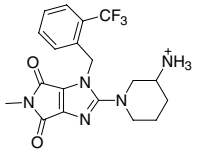	10
11	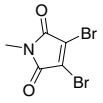	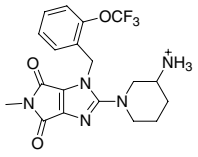	22
12	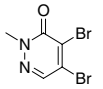	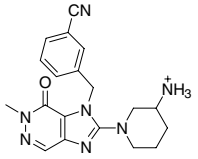	1200
13	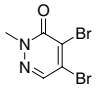	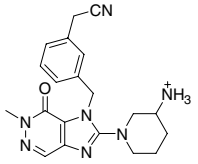	11
14	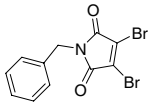	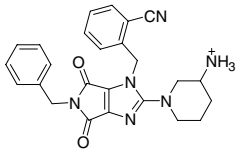	29

Table 1 (*continued*)

Compound	Het	Product	h-DPPIV K_i (nM)
15	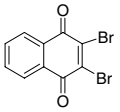	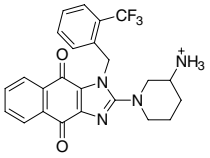	25
16		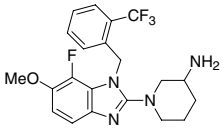	57
17		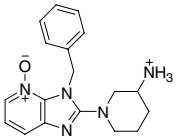	300
18		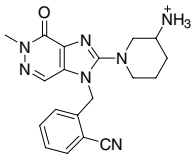	260

The X-ray structure of **7** bound to rat DPPIV (pdb code **2I3Z**) assisted in further rationalizing the SAR by revealing critical binding features necessary for potent DPPIV inhibition (Fig. 3). Analysis of the crystal structure revealed that the 3-amino piperidine was in an ideal position to interact with Glu 203 and Glu 204. The maleimide was oriented to form a π stacking interaction with Tyr 548. The *ortho*-cyano benzyl group is in the vicinity of Ser 631 (the catalytically active serine in DPPIV). Unlike the cyano pyrrolidine DPPIV inhibitors that have been reported in the literature[14,16] there was no direct interaction between the nitrile of **7** and the hydroxyl group of Ser 631. However, the nitrile is being directed to a shallow hydrophobic pocket in P1[14] increasing the inhibitor–protein interaction. This result possibly explains the similar potencies observed when the nitrile was replaced with a chloro or trifluoromethyl group as in **9** and **10** (Table 1). The crystal structure depicts the benzyl group to be orthogonal to the plane of the heterocycle. It is likely that steric and electronic properties of the adjacent carbonyl of the maleimide are contributing to the orthogonality of the benzyl group as predicted by AM1 modeling. Methyl maleimide, **7**, seems to be optimum and larger groups or extensions may be in the way of the protein, as demonstrated by the diminished potency of **14** and **15**.

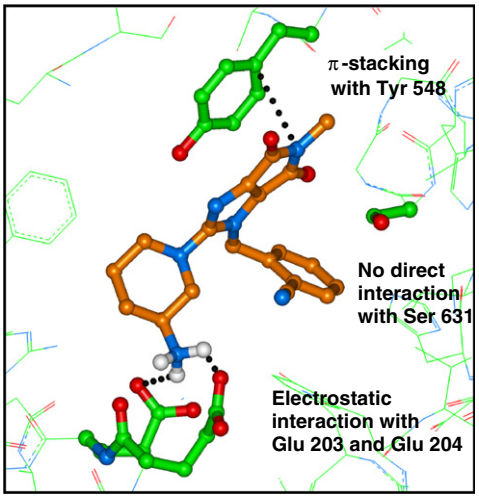

Figure 3. X-ray structure of **7** bound to rat DPPIV.

Compound **7** was unstable in rat plasma and showed a poor pharmacokinetic (PK) profile in Sprague–Dawley

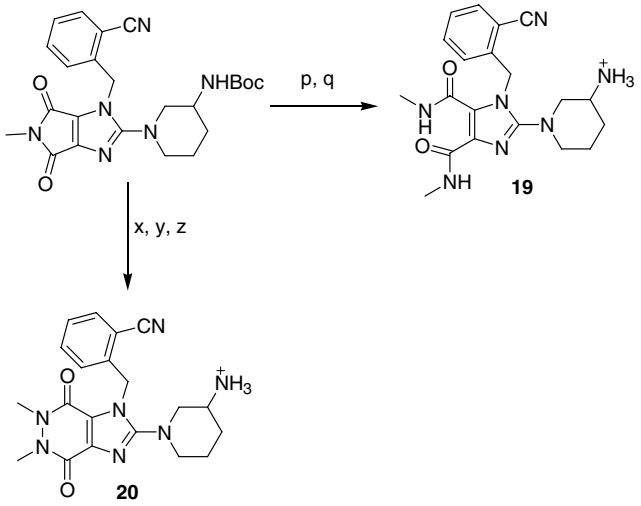

Scheme 2. Reagents and conditions: (p) Methylamine, ACN, 80 °C, 90%; (q) TFA, CH_2Cl_2, 23 °C, 95%. (x) *N*,*N*′-dimethylhydrazine, ACN, 80 °C, 90%; (y) 6N HCl, MeOH, H_2O, 80 °C, 80%; (z) TFA, CH_2Cl_2, 23 °C, 95%.

Table 2. Human and rat DPPIV binding

Compound	h-DPPIV (0% plasma) K_i (nM)	r-DPPIV (0% plasma) K_i (nM)	r-DPPIV (18% plasma) K_i (nM)
6	2	3	7
7	2	2	600
19	450	ND	ND
20	11	17	24

Table 3. Inhibition of other peptidases for selected compounds (K_i = nM)

Compound	DPP8	DPP9	POP
6	>30,000	ND	>30,000
7	>3000	>3000	>30,000
8	>3000	ND	>30,000
13	>3000	ND	>30,000
15	>30,000	>3000	ND
20	>3000	ND	>30,000

rats with a high clearance rate and low oral bioavailability. We reasoned that the low plasma stability was partly due to the electrophilicity of the carbonyl groups which made the maleimide susceptible to nucleophilic attack. In an attempt to make more stable DPPIV inhibitors, **7** was reacted with either N-methyl amine to convert the **A** ring to the ring opened diamide **19** or reacted with *N*,*N*′-dimethylhydrazine to prepare the corresponding pyridazine dione **20** (Scheme 2).

Compounds **7**, **19**, and **20** were tested against human and rat DPPIV enzyme in the presence of 2% and 18% rat plasma to study the effects of plasma stability on DPPIV inhibition (Table 2). Xanthine **6**, maleimide **7**, and pyridazinedione **20** did not show species specificity against human and rat DPPIV enzymes in the absence of plasma. Xanthine **6** is stable in rat plasma with a mere 2-fold shift in potency in the presence of 18% rat plasma (r-DPPIV K_i = 3–7 nM). Confirming the PK and plasma instability result, a significant shift in potency was observed for **7** against DPPIV in the absence of plasma (r-DPPIV K_i = 2 nM) compared to 18% rat plasma (r-DPPIV K_i = 600 nM). The ring opened analog **19** was weak against h-DPPIV. The ring expanded product **20** was 5-fold less potent than **7** (h-DPPIV K_i = 11 nM). However, the compound was stable in rat plasma without a significant shift in potency in the presence of plasma (r-DPPIV K_i = 17–24 nM in 18% plasma).

Human peptidases including DPP7, DPP8, DPP9, and POP are structurally or functionally related to DPPIV and most importantly inhibition of DPP8 and/or DPP9 is associated with significant toxicity.[17] The compounds were screened and found to be inactive against these isozymes (Table 3).

In summary, we have discovered novel, potent, and selective xanthine mimetics based on 5,5 and 5,6 ring fused imidazoles. Compound **7** was found to be a potent and selective DPPIV inhibitor, but it showed a significant loss of activity in the presence of plasma. Compound **20** showed minimal potency changes in the presence of plasma. Hence the shift in potency of **7** was attributed to plasma instability and not protein binding. X-ray analysis of **7** bound to DPPIV indicates that the binding mode is similar to the parent xanthine **6**. Xanthine mimetics allowed us to unravel the key structural features important for potent DPPIV activity while providing good selectivity and no species specificity enabling them to be studied in rodent models of diabetes. These attributes make them excellent compounds to study DPPIV inhibition in vivo as well as assist in designing future DPPIV inhibitors based on this important class of heterocycles.

References and notes

1. Edwards, C.; Mark, B. *Ann. Med.* **2005**, *37*, 314.
2. Meier, J. J.; Nauck, M. A. *Horm. Metab. Res.* **2004**, *36*, 859.
3. Holst, J. J.; Gromada, J. *Am. J. Physiol. Endocrinol. Metab.* **2004**, *47*, 357.
4. Fehmann, H. C.; Habener, J. F. *Endocrinology* **1992**, *130*, 2890.
5. Heller, R. S.; Kieffer, T. J.; Habener, J. F. *Diabetes* **1997**, *46*, 785.
6. Imeryuz, N.; Yegen, B. C.; Bozkurt, A.; Coskun, T.; Villanueva-Penacarrillo, M. L.; Ulusoy, N. B. *Am. J. Physiol.* **1997**, *273*, G920.
7. Egan, J. M.; Bulotta, A.; Hui, H.; Perfetti, R. *Diabetes Metab. Res. Rev.* **2003**, *19*, 115.
8. Orville, G.; Kolterman, J. B.; Buse, J. B.; Fineman, M. S.; Eling, G.; Sonja, H.; Bicsak, T. A.; Taylor, K.; Kim, D.; Aisporna, M.; Wang, Y.; Baron, A. D. J. *Clin. Endocrinol. Metab.* **2003**, *88*, 3082.
9. Weber, A. *J. Med. Chem* **2004**, *47*, 4135.
10. Augustyns, K.; Van der Veken, P.; Haemers, A. *Expert Opin. Ther. Patents* **2005**, *15*, 1387.
11. Szczepankiewicz, B. G.; Kurukulasuriya, R. *Curr. Top. Med. Chem.* **2006**, in press.
12. Gwaltney, S. L.; Aertgeerts, K.; Feng, J.; Kaldor, S. W.; Kassel, D. B.; Manuel, M.; Navre, M.; Prasad, S. G.; Shi, L.; Skene, R. J.; Stafford, J. A.; Wallace, M.; Xu, R.; Ye, S.; Zhang, Z. *Abstracts of Papers*, 231st Meeting of the American Chemical Society, Atlanta, GA, 2006; MEDI-018.
13. Kanstrup, A. B.; Christain, L. B.; Lundbeck, J. M.; Sams, C. K.; Kristiansen, M.; WO Patent 0202560, 2001.
14. Longenecker, K. L.; Stewart, K. D.; Madar, D. J.; Jakob, C. G.; Fry, E. H.; Wilk, S.; Lin, C. W.; Ballaron, S. J.; Stashko, M. A.; Lubben, T. H.; Yong, H.; Pireh, D.; Pei, Z.; Basha, F.; Wiederman, P. E.; von Geldern, T. W.; Trevillyan, J. M.; Stoll, V. S. *Biochemistry* **2006**, *45*, 7474.
15. Szczepankiewicz, B. G.; Rohde, J. J.; Kurukulasuriya, R. *Org. Lett.* **2005**, *7*, 1833.
16. Engel, M.; Hoffman, T.; Wagner, L.; Wermann, M.; Heiser, U.; Kiefersauer, R.; Huber, R.; Bode, W.; Demuth, H. U.; Brandstetter, H. *PANS* **2003**, *100*, 5063.
17. Lankas, G.; Leiting, B.; Roy, R. S. *Diabetes* **2004**, *53*, A2-OR.